Heliyon 9 (2023) e19709

Contents lists available at ScienceDirect

Heliyon

journal homepage: www.cell.com/heliyon

Simple solutions for improving thermal comfort in huts in the highlands of Peru

Enrique Mejia-Solis [a,b,*], Jaime Arias [a], Björn Palm [a]

[a] Department of Energy Technology, Royal Institute of Technology KTH, SE-100 44 Stockholm, Sweden
[b] GRUPO de Apoyo al Sector Rural de la Pontificia Universidad Católica del Perú, Peru

ARTICLE INFO

Keywords:
Building performance simulation
Low indoor temperatures
Uncertainty analysis
Andes
Low-cost refurbishments

ABSTRACT

In the Peruvian mountains, hundreds of thousands of rural households living in poverty live in cold indoor environments, close to 0 °C. Indoor cold causes thousands of respiratory diseases and excess of winter deaths. In this study, we numerically calculated the impact of simple low-cost refurbishments on discomfort time during a year.

Using EnergyPlus and Python, we modelled a typical one-room hut used as bedroom built with a metal-sheet roof, adobe walls, dirt floors, and high infiltration rates. Then, 9 individual solutions were studied, and their combination resulted in 215 different hut designs. The model was calibrated with field measurements to estimate the infiltration. All the numerical calculations included an uncertainty analysis based on Monte Carlo method, and a sensitivity analysis to assess the impact of reducing infiltration on discomfort time.

The base case had a discomfort time of 44% of time. The calibration of infiltration resulted in a mean hourly air exchange rate equal to 29.1 h^{-1} (SD = 17.0 h^{-1}). Five different designs formed the Pareto front that optimized discomfort time and costs. The solution with the lowest discomfort time during a year, 37% of the time, was adding insulation to the roof (U = 0.83 W/m^2•K) and the door (U = 1.00 W/m^2•K); and its cost was 286USD. In this solution, when infiltrations were reduced to 4.1 h^{-1} (SD = 4.1 h^{-1}) discomfort time decreased until 16%.

These results benefit those households that nowadays invest their limited resources to improve their living conditions but without technical guidance.

1. Introduction

In the Peruvian mountains, nighttime indoor temperatures in rural houses are as low as 1 °C [1–3]. Most houses are mud-brick huts with a thin metal roof, a thin metal door, and bare soil as a floor, and they exhibit high air leakage through holes in the windows, doors, and/or roofs [2,4–6] (Fig. 1 & Fig. 2). Low indoor temperatures are related to cardiovascular problems, mental health disorders, respiratory infections, and excess winter mortality [3,7]. These effects are also related to other local risk conditions such as low socioeconomic status, vulnerability to outdoor winter temperatures, difficulty accessing health services, and indoor air contamination caused by dirt floors and cooking smoke [8]. All the risk conditions mentioned contribute to thousands of respiratory infections and hundreds of deaths among vulnerable people each winter [3,8].

To describe local demographics and housing conditions, we used data from Peru's 2019 National Demographic and Health Survey

* Corresponding author. Department of Energy Technology, Royal Institute of Technology KTH, SE-100 44 Stockholm, Sweden.
E-mail addresses: enr@kth.se (E. Mejia-Solis), jaime.arias@energy.kth.se (J. Arias), Bjorn.Palm@energy.kth.se (B. Palm).

https://doi.org/10.1016/j.heliyon.2023.e19709
Received 30 May 2022; Received in revised form 28 April 2023; Accepted 30 August 2023
Available online 12 September 2023
2405-8440/© 2023 Published by Elsevier Ltd. This is an open access article under the CC BY-NC-ND license (http://creativecommons.org/licenses/by-nc-nd/4.0/).

Fig. 1. (a) Household settlement formed by multiple huts and (b) typical mud-brick hut in the rural Peruvian mountains.

[9]. This survey was a sample survey designed according to an internationally known methodology [10]. We calculated that approximately 2.8 million people, a number which represents 9% of the total Peruvian population [11], lived in the rural mountains and were distributed in 990,000 households, which represents 12% of the total households in Peru [11]. 87% of these households lived in buildings that used mud or mud bricks as the main wall material, 66% lived in buildings that had a roof made of metal sheet roofing, fiber cement, or a similar material, 75% lived in buildings that had dirt floors, and 75% used biomass for cooking. 90% of the households that used biomass for cooking had a room specially designated for cooking, which is possible evidence that the use of biomass for heating is rare.

Between 2017 and 2019, the Peruvian government invested close to 150 million USD to refurbish more than 6300 houses [12]. The government installed wooden floors, ceilings, new windows, small vestibules, and a Trombe wall for passive solar heating (Fig. 3b). In a refurbished house at 4 a.m., the indoor temperature was 16 °C and the outdoor temperature was −1 °C (building layouts and number of occupants were not reported) [13]. In addition, between 2019 and 2020, the government invested approximately 190 million USD to build 24,370 houses [8]. These houses had an area of 33 m^2, with two bedrooms, one living room, an insulated envelope, double-glass windows, adobe or fired-brick walls, but no heating system [1] (Fig. 3a). In one house, nighttime indoor temperatures were between 6 °C and 9 °C, while outdoor temperatures were between 2 °C and 7 °C (the number of occupants during these measurements was not reported) [1]. Private institutions have also financed hundreds of house improvements [14]. Despite all these investments, thousands of households still need warmer houses.

Local professionals have studied low-cost passive solutions using local materials to increase thermal insulation, airtightness, and solar heat gains (winter solar radiation is relatively high) (Table 1) [15–18]. Weiser et al. [16] numerically calculated the impact of using different construction materials on indoor temperatures in a 14.8 m^2 one-room house. They tested: (1) fired clay brick walls with concrete roof; (2) adobe walls with wooden roof; (3) light earth wall (0.12 m thickness) with light earth roof; and (4) light earth wall (0.22 m thickness) with light earth roof. The most comfortable combination was light earth wall (0.22 m thickness) with light earth roof and it was comfortable during 94% of the time during winter. The researchers used the adaptive thermal comfort model defined by De Dear & Brager [19].

Other local professionals have studied low-cost mechanical heating systems. Molina et al. [6] tested a system made of a solar thermal collector, and a 65-L radiator made of 6-inch diameter PVC tube. Warm water flowed from the solar collector at 6 p.m. to the

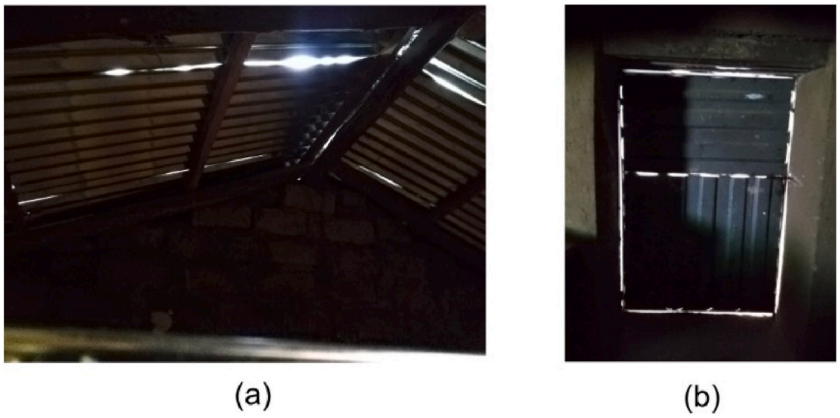

Fig. 2. Air leakage through a (a) roof, and (b) door.

Fig. 3. Houses (a) newly built or (b) refurbished as part of public housing programs.

Table 1
State of the art of passive constructive solutions in Peru [15].

Fenestration	Roof insulation	Wall insulation	Floor insulation	Increased solar heat gain
Windows: • Double glazing (air cavity), wood frame, mud to cover joints. • Opaque shutters for nighttime use. Door: • Vestibule. • Doors with two layers of wood with cavity insulation (expanded polystyrene).	• Plywood ceiling with insulation made of straw (ichu) • Woven polyethylene fabric ceiling, with straw (ichu) sparsely strewn over it as insulation. • Reed (totora) ceiling covered with plaster. • Three-layer roof material: exterior layer of cement, sheep wool as insulation, and interior layer of zinc roofing. Mud to cover the joints. • Three-layer roof material: exterior zinc roofing, an air space, and interior insulation made of reeds (totora). • Three-layer roof material: exterior zinc roofing, expanded polystyrene, and interior plywood.	• Exterior insulation made of a layer of reeds (totora) installed using mud and straw. • Walls made of two adobe wall layers with air as a cavity insulation.	• Three-layer floor: (bottom) stones, air space, and (upper) wood. • Three-layer floor: (bottom) stones, mud with straw, and (upper) mud with sand. • Four-layer floor: (bottom) plastic sheet, expanded polystyrene, air space, and (upper) wood flooring.	• Polycarbonate skylight(s) with plywood shutters. • Two greenhouses made of transparent plastic sheet and attached to the west and east sides. • Attached greenhouse made of adobe walls and semitransparent plastic sheet roof. The wall connecting the greenhouses and the house has openings to let the air circulate naturally during daytime hours. • Naturally ventilated Trombe wall inclined 70°.

PVC tube and stayed there until 6 a.m. The test was done in a 9 m^2 × 2.2 m room with adobe walls, double doors, insulated floor, insulated roof, and double-glazed windows with shutters. Indoor temperatures went from 14 °C to 12 °C while nighttime outdoor temperatures went from 7 °C to 0 °C. Holguino et al. [20] studied latent heat storage in a floor made with four layers: a bottom layer of concrete; a layer of insulation; a layer of andesite stone with guano, as a heat-storage material; and an upper layer of wood. Warm water ran through tubes in the floor. The test was done in an empty 4.6 m^2 × 1.7 m room with adobe walls, double-glazed windows, plywood ceiling, insulated roof, and insulated walls. Nighttime indoor temperatures went from 10 °C to 6 °C while outdoor temperatures went from 5 °C to −2 °C.

Similar housing problems affect people in other mountainous regions of the world with similar social conditions. In Ecuador, Miño-Rodriguez et al. [21] calculated that the indoor temperature in a low-cost house during a year dropped to a minimum of 3.3 °C and had a median temperature of 6.1 °C, while the minimum outdoor temperature was 1.9 °C. This one-story house had an area of 34 m^2, a roof made of concrete tiles, a floor made of concrete with plaster, and walls made of compressed stabilized earth blocks. The researchers calculated that mounting a ceiling and reducing air infiltration increased the minimum temperature by 0.9 °C and the median by 1.7 °C. In Nepal, Thapa et al. [22] measured a mean nighttime indoor temperature of 10.3 °C in temporary shelters made of metal sheets while the mean outdoor temperature was 7.6 °C. The researchers numerically calculated that adding a 2 mm tarpaulin and 12 mm cellular polyethylene foam to walls and roofs raised indoor temperatures over 11 °C for 70% of the night.

People living at high altitudes and with low indoor temperatures feel more satisfied with their indoor environment at lower temperatures than other populations living in more conventional conditions [23]. Mountainous populations living in cold houses have developed behavioral adaptations to the cold and expect to feel cold indoors [24]; these two characteristics help them to feel comfortable at lower temperatures [25]. For this reason, conventional thermal comfort models, like Fanger's Predictive Mean Vote (PMV) or ASHRAE's adaptive thermal comfort model, predict higher cold discomfort than the discomfort found in field studies focused on mountainous populations [23,26,27]. Furthermore, laboratory comfort models like the PMV do not include the influence of

hypobaric conditions in the heat transfer between humans and the indoor environment [28].

In the Peruvian mountains, 46% of 10 people surveyed were satisfied in rooms with air temperatures between 5 °C and 12 °C [29]. However, the studied sample was arguably small, 10 people, to be used to generalize the results for the entire territory. In another study, 32 out of 43 households belonging to a public housing program (Fig. 3a) were satisfied with their indoor environment [30]. The researcher did not measure indoor temperatures but, according to another report, the mean nighttime indoor temperature could have been 7 °C [1].

Other mountainous populations also feel thermally satisfied at low indoor temperatures. In rural stone dwellings in Tibet, 76% of 327 people surveyed were satisfied with operative temperatures between 3.5 °C and 7.5 °C, while outdoor temperatures were between −5.6 °C and 10.3 °C [27]. In that survey, the calculated neutral temperature, defined using linear regression, was 12.9 °C. In Nepal, in temporary shelters made of zinc sheets, 46% of 695 people surveyed were satisfied with their indoor environment when indoor air temperatures were between 5 °C and 29 °C and outdoor temperatures were between 1 °C and 25 °C [31]. The winter neutral temperature, calculated using Griffiths' method, was between 15.0 °C and 20.8 °C depending on the region.

We have observed that some households in the Peruvian mountains have invested in refurbishments to increase indoor temperatures. These include reducing infiltrations, installing woven polyethylene ceilings, and/or installing semitransparent plastic sheets as skylights (Fig. 4). A household will implement solutions based on empirical experience, but empirical evidence could be misleading. For example, skylights could be too small to cause a significant impact on nighttime temperatures. Thus, empirical decisions need to be supported by scientific evidence to guarantee that households can use their limited resources effectively. This scientific evidence must consider a variety of conditions such as house size, number of occupants, and weather. This evidence is rarely found in the literature.

In this study, we evaluated simple low-cost refurbishments such as skylights and insulation, either as stand-alone or combined solutions. The main objective was to find which solution had the greatest impact on thermal comfort. The perceived comfort was numerically calculated including an uncertainty analysis. The impact of reducing infiltration in a refurbishment was calculated via a sensitivity analysis.

Sensitivity analysis has been seldom applied in the thermal analysis of buildings located in tropical weathers and at high-altitude, like in our case of study. Two particular characteristics of this weather are high solar radiation during winter and high daily temperature oscillation during the whole year. Ordóñez et al. [32] did a sensitivity analysis of a 36 m^2 unconditioned dwelling located in Quito i.e. tropical weather and at 2800 m. They used a calibrated model and different boundary conditions to study the influence on thermal comfort of five parameters: windows to wall ratio, air infiltration, window orientation, window glazing, and envelope's thermal mass. The researchers found that window to wall ratio was the most sensitive parameter and a range from 20 to 40% resulted in the highest number of hours with thermal comfort. Window orientation and window glazing had the lowest influence.

We consider this study to be a contribution not only to the inhabitants, for the reasons already explained, but also to science. Uncertainty and sensitivity analyses of building performance simulations is a research area that has been getting more attention in the last two decades [33]. However, these analyses are often done on conventional buildings. In our study, we focused on the uncertainties of construction materials and other conditions that are not common in the literature and looked at secondary sources uncommon in other building performance simulations.

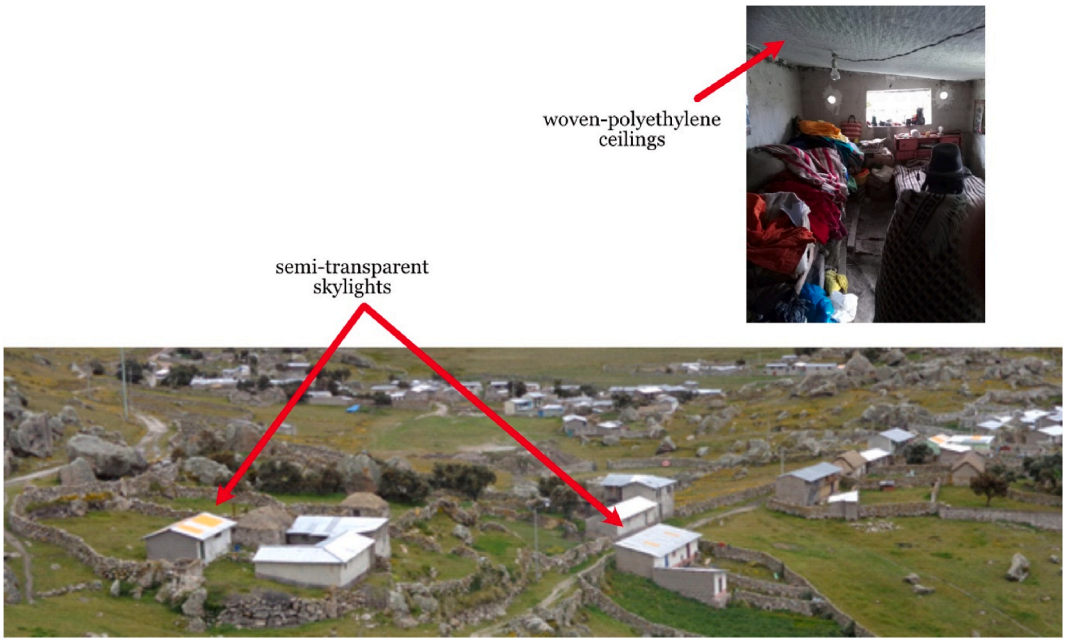

Fig. 4. Evidence of refurbishments.

2. Methodology

Numerical calculations were performed using EnergyPlus v22.2., a building energy simulation program [34]. First, a base case building was defined, and 9 refurbishment solutions based on passive techniques were selected from the literature. Then, these solutions were combined to create 215 new building designs. Nighttime operative temperatures and comfort indices were then calculated for each design, with nighttime being considered the time between 8 p.m. and 5 a.m. The calculations were performed with a frequency of 1 h for one year. The calculations included an uncertainty analysis using a Monte Carlo analysis.

To assess the impact of including a refurbishing solution in a building design, a sensitivity analysis was performed based on linear regression and the calculation of standard regression coefficients (SRC).

The Python programing language and the Eppy library (https://pypi.org/project/eppy/) were used for the parametric analysis with EnergyPlus, for the Monte Carlo analysis, and for the multivariable linear regression and SRC calculations.

2.1. EnergyPlus's model

EnergyPlus uses the heat balance method to do transient heat transfer calculations assuming indoor air is at the same temperature throughout the entire volume of a thermal zone. It also assumes the existence of uniform surface temperatures, uniform irradiation, diffuse radiation, and one-dimensional heat conduction [34,35]. This method analyzes four processes: heat balance at the walls' outdoor surfaces, heat conduction through the walls, heat balance at the walls' indoor surfaces, and indoor-air heat balance. The indoor-air heat balance is the distribution of heat supplied to the thermal zone's indoor air. In a zone without mechanical heating or ventilation, the indoor-air heat balance was [36]:

$$\text{energy stored in zone air [J/s]} = \text{sum of convective internal loads [J/s]} + \text{convective heat transfer from zone surfaces [J/s]} + \text{heat transfer caused by air infiltration [J/s]}$$

$$\rho_z V c_p \frac{dT_z}{dt} = \sum_{i=1}^{N_{sl}} \dot{Q}_i^t + \sum_{i=1}^{N_{surfaces}} h_i^t A_i \left(T_{si}^t - T_z^t\right) + \dot{m}_{inf}^t c_p \left(T_\infty^t - T_z^t\right) \quad (1)$$

where

A_i = area of the zone surface i [m^2]
c_p = specific heat of the air [J/(kg•K)]
h_i^t = convective heat transfer coefficient at time t [W/(m^2•K)]
$\dot{m}_{inf}^t$ = air infiltration mass flow rate [kg/s]
N_{sl} = number of convective internal loads [−]
$N_{surfaces}$ = number of surfaces in the thermal zone [−]
$\dot{Q}_i^t$ = heat flux from source of internal load at time t [J/s]
T_{si}^t = temperature of surface i at time t [K]
T_z^t = indoor air temperature at time t [K]

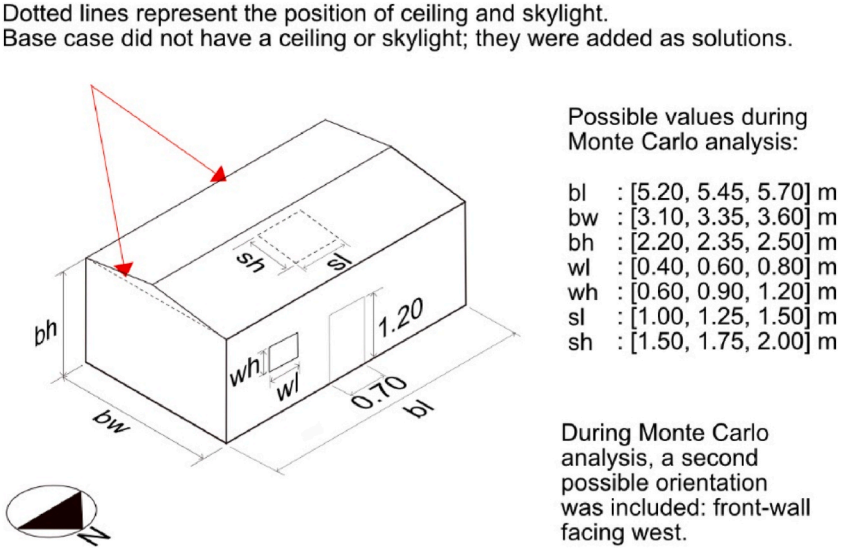

Fig. 5. Base case model geometry, dimensions, and orientation.

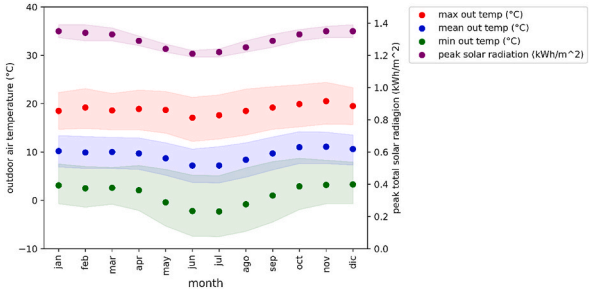

Fig. 6. Distribution of outdoor temperatures and solar radiation of typical meteorological years generated for 557 districts over 3500 m. a.s.l. Mean values, percentiles 5th, and percentiles 95th are shown.

Table 2
Description of base case and retrofitting solutions.

Category	Options
Skylight	s1. Base case: No skylight s2. Adding skylight: material = PVC with yellow pigment; thickness = [0.003, 0.004, 0.005] m; area = 1 m^2; U_{min} = 34.00 W/m^2•K; U_{max} = 56.67 W/m^2•K; cost = 26 USD s3. Adding skylight and shutters: Skylight same as s2. Shutter outside layer material = plywood; thickness = 0.004 m; middle layer material = EPS; thickness = 0.04 m; inside layer material = plywood; thickness = 0.004 m; U = 0.83 W/m^2•K; cost = 78 USD
Roof	r1. Base case: material = metal roofing; thickness = 0.00022 m; U = 205909.09 W/m^2•K r2. Adding insulated roof: outside layer material = metal roofing; thickness = 0.00022 m; inside layer material = EPS; thickness = 0.04 m; U = 0.83 W/m^2•K, cost = 260 USD r3 Adding a lightweight ceiling: outside layer material = metal roofing; thickness = 0.00022 m; middle layer material = air; thickness = 0.143 m; inside layer material = woven polypropylene; thickness = 0.002; U = 5.85 W/m^2•K, cost = 130 USD
Door	d1 Base case: material = metal roofing; thickness = 0.00022 m; U = 205909.09 W/m^2•K d2 Adding insulated door: outside layer material = plywood; thickness = 0.004 m; middle layer material = EPS; thickness = 0.03 m; inside layer material = plywood; thickness = 0.004 m; U = 0.83 W/m^2•K; cost = 26 USD
Floor	f1 Base case: material = dry soil; thickness = 0.001 m; U = 500.00 W/m^2•K f2 Adding insulated floor: outside layer material = EPS; thickness = 0.005 m; inside layer material = wood; thickness = 0.019 m; U = 3.26 W/m^2•K, cost = 520 USD
Window	wi1 Base case: material = clear glass; thickness = [0.003, 0.004, 0.005] m; U_{min} = 280.00 W/m2•K; U_{max} = 466.67 W/m2•K wi2 Adding shutters: outside layer material = plywood; thickness = 0.004 m; middle layer material = EPS; thickness = 0.003 m, inside layer material = plywood; thickness = 0.004 m; U = 1.00 W/m^2•K; cost = 26 USD.
Walls	wa1 Base case: material = adobe; thickness = [0.30, 0.35, 0.40] m; U_{min} = 0.71 W/m^2•K; U_{max} = 2.67 W/m^2•K wa2 Adding interior insulation: outside layer = adobe; thickness = [0.30, 0.35, 0.40] m; inside layer = EPS; thickness = 0.02 m; U_{min} = 0.49 W/m^2•K; U_{max} = 1.00 W/m^2•K; cost = 260 USD wa3 Adding exterior insulation: outside layer = EPS; thickness = 0.02 m; inside layer = adobe; thickness = [0.30, 0.35, 0.40] m; U_{min} = 0.49 W/m^2•K; U_{max} = 1.00 W/m^2•K; cost = 260 USD

Note: U_{min} and U_{max} are the minimum and maximum values in all the combinations done during the Monte Carlo analysis. Thickness values in brackets are the possible values during the Monte Carlo analysis.

T^t_∞ = outdoor air temperature [K]
V = volume of the thermal zone [m^3]
ρ_z = air density [kg/m^3]
Air infiltration rate (V_{inf}) was calculated using:

$$V^t_{inf} = \frac{A_L}{1000}\sqrt{C_s(\Delta T^t) + C_w(U^t)^2} \quad (2)$$

V_{inf} = air infiltration rate at time t, m^3/s
A_L = effective air leakage area, cm^2

Table 3
Properties of opaque materials.

Material name	metal roofing (zinc-coated steel)	Dry Soil & ground	Wood floor (oak)	Expanded polystyrene	Woven Polypropylene	Plywood (pine)
Roughness	Smooth	Rough	Rough	Rough	Rough	Rough
Conductivity (W/m•K)	45.3 [35]	0.5 [47]	0.176 [35]	0.038 [48]	0.24 [49]	0.092 [35]
Density (kg/m^3)	7830 [35]	1200 [47]	750 [35]	23 [48]	905 [49]	370 [35]
Specific heat (J/kg•K)	500 [35]	1000 [47]	2390 [35]	1500 [48]	1930 [49]	1880 [35]
Thermal absorptance (–)	0.3 [50]	0.9 [38]	0.9 [51]	0.88 [51]	0.88 [51]	0.9 [51]
Solar absorptance (–)	0.38 [50]	0.4 [38]	0.38 [51]	0.2 [51]	0.2 [51]	0.38 [51]

Table 4
Thermal properties of adobe bricks.

Set of properties		Thermal conductivity W/(m•K)	Specific heat capacity J/(kg•K)	Density kg/m3
International references [53–55]	set 1	0.519	1005	1696
	set 2	0.560	837	1922
	set 3	0.800	1000	1600
Peruvian reference [56]	set 4	0.316	613	1766
	set 5	0.283	609	1716
	set 6	0.312	587	1701

$$C_s = \text{stack coefficient, } (\text{L/s})^2 \Big/ \left(\text{cm}^4 \bullet \text{K}\right)$$

ΔT^t = indoor (T_i^t) – outdoor (T_o^t) temperature difference at time t, K

$$C_w = \text{wind coefficient, } (\text{L/s})^2 \Big/ \left[\text{cm}^4(\text{m/s})^2\right]$$

U^t = local wind speed at time t, m/s

The values of C_s and C_w, respectively, were 0.000319 and 0.000145, taking into account a one-story building with no obstacles around it [35]. A_L was randomly selected from a probability distribution explain in the *Model calibration and infiltration* section below.

Foundation: The *Kiva* model was used to calculate heat transfer to the ground. It performs two-dimensional finite difference calculations using information regarding the building layout, weather, sun position, zone temperatures, and zone radiation [37]. An adiabatic boundary condition under the ground at a depth of 14 m was assumed [38].

The TARP model was used to calculate convective heat transfer coefficients with internal surfaces, which considers surface orientation and temperature difference [36]. The DOE-2 model was used to calculate convective heat transfer coefficients with external surfaces, which considers surface orientation, temperature difference, surface roughness, and wind speed [36].

2.2. Base case, retrofitting solutions, and uncertainty analysis

The base case model was a detached bedroom with a typical building layout (Fig. 5) and construction materials [4,39] (Fig. 6). To define the base case, EnergyPlus required inputs related to the physical properties of the construction materials, the building layout, infiltration, internal heat gains, and weather. Nine refurbishing solutions were selected to modify the base case (Fig. 6): adding a skylight, adding a lightweight ceiling, adding window or skylight shutters that were closed during the night, and adding insulation to

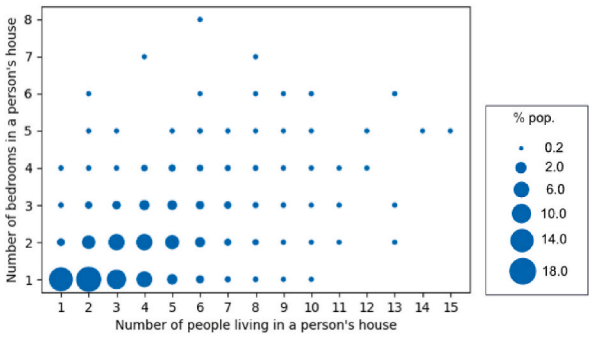

Fig. 7. Percentage of the rural population in the Peruvian mountains grouped by number of bedrooms in each house and number of household members according to Peru's 2019 National Demographic and Health Survey.

Table 5
Properties of glazing materials. Values were selected from the uniform probability distributions in the brackets.

Material properties	Clear glass	PVC with yellow pigment (derived from properties of clear PVC [62–64])
Solar transmittance at normal incidence	[0.83 [35], 0.70, 0.58]	[0.87, 0.73, 0.60]
Front/Back side solar reflectance at normal incidence	[0.08 [35], 0.07, 0.06]	[0.09, 0.08, 0.07]
Visible transmittance at normal incidence	[0.90 [35], 0.76, 0.63]	[0.87, 0.73, 0.60]
Front/Back side visible reflectance at normal incidence	[0.08 [36]. 0.07, 0.06]	[0.10, 0.09, 0.08]
Infrared transmittance at normal incidence	0 [36]	[0.07, 0.05, 0.04]
Front/Back side infrared hemispherical emissivity	[0.92 [67], 0.93, 0.94]	[0.75, 0.78, 0.80]
Thermal conductivity (W/m•K)	1.4 [67](±5%)	0.17(±5%)

the roof, door, floor, interior surface of walls, or exterior surface of walls (Table 2). In the case of the solutions that included to add insulation to the envelope, insulation was added until complying with Peruvian standards for minimum U-values in this kind of weather: $U_{walls} \leq 1.00$ W/m^2•K, $U_{roof} \leq 0.83$ W/m^2•K, $U_{floor} \leq 3.26$ W/m^2•K [40]. Calculation of each solution cost included construction material costs and manufacturing (Table 2). These solutions were combined using full-factorial design, which resulted in 215 new building designs.

Each of the 215 new house designs and the base case were defined by a set of inputs necessary for the calculations. The value of each input was randomly selected from probability distributions following the Monte Carlo methodology. According to this methodology, a random selection is performed for each input more than one time; thus, each design was represented by various sets of inputs with randomly selected values. All calculations were performed for each set of inputs. Several tests were run, and it was concluded that 200 sets of inputs per design resulted in consistent outputs.

The probability distributions related to inputs about thermophysical properties were normal distributions with standard deviations (SD) of 5% (Table 3), as is usually the case in uncertainty analyses of building performance simulations [33,41–46]. In this study, the maximum value for the absorptance properties was set to 0.95. For inputs related to building dimensions, building orientation, and material thickness, uniform probability distributions were used, and their values are indicated inside brackets in Fig. 5 & Table 2. Uniform probability distributions are also common in uncertainty analyses of building performance simulations [33,41–46]. Inputs needing further explanation were weather, the adobe's thermophysical properties, the internal heat gains and mass, and the glazing materials' thermophysical properties.

a) Weather

The Peruvian mountains is classified in two regions according to the altitude [52], the highest altitude region, above 3500 m. a.s.l. was chosen for this study. According to the national census of 2017, there are 557 districts with rural population living in huts. Typical meteorological years weather files were created with Meteonorm 7.2 for these districts. These files show that, in this region, outdoor temperature variation along the year is low but during a day is high, and there is high solar radiation during the whole year (Fig. 6), During the Monte Carlo analysis, each weather file had the same probability of being included as an input.

b) Adobe's thermophysical properties

Adobe bricks have different thermal properties depending on their manufacturing process. In Peru, adobe bricks are made artisanally, and their thermal conductivities and specific heat capacities are lower than international references (Table 4). During the Monte Carlo analysis, each of the sets of properties shown in Table 4 had the same probability of being included as an input. In each set, solar and thermal absorptances were 0.94 and 0.70, respectively. Each property was assigned a normal probability distribution with an SD of ±5%, but the maximum admitted value for absorptance was 0.95.

c) Internal heat gains and mass

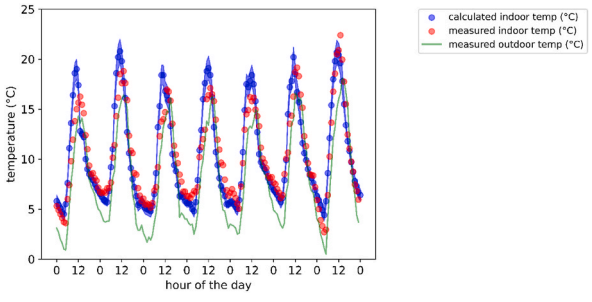

Fig. 8. Calculated indoor air temperatures inside a hut after model calibration and measured indoor air temperatures. For the calculation, a point is the mean values, and shadowed area is the distribution between percentiles 5th and 95th.

One person was assumed to be indoors all day, and that it would open the door, which increased the infiltration, when indoor air temperature was higher than 14 °C. This temperature was chosen assuming that these people feel comfortable at relatively low temperatures as studies in Nepal [57]. Additional people were assumed to be indoors between 8 p.m. and 5 a.m. in some cases. To estimate the number of people sleeping in the room, data from Peru's 2019 National Demographic and Health Survey [39] was used to calculate the number of bedrooms and household members per household (Fig. 7). Most households had 1 or 2 bedrooms, and 1 to 5 members. Thus, the input *number of people sleeping in a bedroom* had a uniform probability distribution with values of 1, 2 or 3. The heat production of each person was selected from a normal probability distribution with a mean of 70 W and an SD of 10%.

The people's total thermal insulation due to clothing, bed clothes, and type of bed was selected from the uniform probability distribution [3.3, 3.8, 4.3] clo. These were selected taking into account our observations and results from experimental measurements in the literature [58].

One light bulb was assumed as other internal gain, it was incandescent and turned on from 8 p.m. to 9 p.m., with a heat production of 50 W, and radiant and visible fractions equal to 0.8 and 0.1, respectively [59].

Internal mass was considered to be furniture modelled as a wood sheet measuring 4 m^2 × 0.013 m.

d) Glazing material

The glazing materials' optical properties were assumed to be affected by soiling, decreasing transmittance down to 70% and reflectance down to 85% of their respective nominal values [60,61], thus increasing emissivity (Table 5). The properties of Polyvinyl chloride(PVC) with yellow pigment were derived from those of PVC without pigments [62–64], assuming that yellow pigment reduced transparency by 96% [65] and mainly increased reflectance [66].

2.3. Model calibration and infiltration

A calibration of the EnergyPlus model using field measurements was used to find adequate values of air infiltration. Air infiltration in similar buildings has been registered in the literature but in a broad range of values. Williams & Unice [5] measured infiltrations in two houses in the Peruvian mountains using a tracer gas technique. These two houses were two-story buildings with higher-quality construction than that of our base case. AERs were from 0.5 h^{-1} to 6.2 h^{-1} with closed windows. In the Guatemalan mountains, researchers studied a hut used as kitchen and calculated AER between 7.3 h^{-1} to 52.9 h^{-1} using the rate at which particles of carbon monoxide were removed [68,69]. Considering that infiltration is one of the most influential parameters in the calculation of indoor temperatures in similar buildings [32], a model calibration was done using physical measurements.

Two air temperature sensors (Elitech RC-4HC) were placed inside a hut in Langui district in Cusco, Peru (Fig. 1b). Outdoor environmental conditions were measured with a meteorological station (monitoring station Onset HOBO RX3004, solar radiation sensor Onset HOBO S-LIB-M003, air temperature/relative humidity sensor Onset HOBO S-THC-M002, Davis wind speed and direction sensor S-WCF-M003). Measurements were done for 8 days (from the 14th to the 21st October 2022) and data was averaged to 1-h bins to be consistent with our simulations results, which were done with 1-h frequency (Fig. 7).

The measured weather data were used to calculated indoor air temperatures inside the hut. This calculation included an uncertainty analysis of the thermophysical properties of the materials. The materials' thermophysical properties were randomly sample 100 times creating 100 different simulation files. Each file was simulated 20 times with different effective air leakage area (A_L in Eq (2)) values from 2000 to 7000 cm^2 with increments of 250 cm^2. For each A_L the Normalized Mean Bias Error (NMBE) and Normalized Root Mean Square Error (NRMSE) was calculated. For each file, A_L that minimized NMBE was selected; in all cases, the values of NMBE and NRMSE were lower than those recommend in the literature, 5% and 10% respectively [32].

2.4. Thermal comfort model

Rijal has extendedly studied thermal comfort of people living in high altitude mountains in Nepal and in similar housing conditions than those described in the present study [22,31,57,70–72]. An adaptive thermal comfort model developed by Rijal [57] was chosen for this study to calculate comfort temperatures (T_c), which are temperatures that cause a neutral thermal sensation. The model is:

$$T_c = 0.808 T_g + 4.4°C \quad (3)$$

T_g = globe temperature (°C)

T_g was assumed equal to the operative temperature T_o calculated by Energy Plus. The comfortable range for 80% of acceptability was defined as $T_c \pm 3.5$ °C [73].

2.5. Optimal solutions and infiltration sensitivity analysis

Optimal solutions were the set of all retrofitting solutions in the Pareto front of two variables: investment costs (Table 2) and discomfort time during a year. Discomfort time was defined as the total number of hours of the year when indoor air temperatures were outside the comfortable range. This total number of hours was calculated adding all the results for each of the 200 sets of inputs per design. The discomfort time during a year was expressed as a percentage over the total number of hours during a year (8760).

Sensitivity analysis was applied to study the effect of reducing infiltration in the optimal solutions and the base case. Reducing

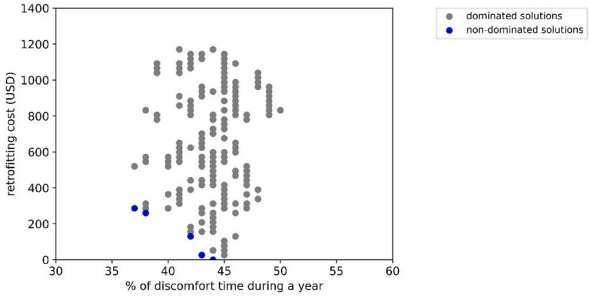

Fig. 9. Pareto front formed with the set of designs that optimize cost and discomfort. The point with zero investment is the base case.

Table 6
List of designs in the Pareto front of cost and discomfort.

Design	Investment cost (USD)	% of discomfort time during a year
Base case	0	44
Adding insulated door	26	43
Adding shutters	26	43
Adding lightweight ceiling	130	42
Adding insulated roof	260	38
Adding insulated roof and adding insulated door	286	37

infiltration was not included as a retrofitting solution because of its difficulty to control its implementation in real life, and lack of data of infiltration in this kind of building. Thus, this sensitivity analysis was included to assess the potential reduction in discomfort if measures to reduce infiltration were possible.

3. Results

The maximum and minimum measured indoor temperature were 22.4 °C and 2.7 °C, respectively (Fig. 8). Indoor temperature oscillation between day and night was close to the outdoor temperature oscillation (Fig. 8). Around noon, indoor temperatures were higher than outdoor temperatures because of the high thermal transmissivity of the metal roof.

Model calibration in combination with an uncertainty analysis resulted in 100 values of air effective leakage area (A_L). These 100 values were approximately distributed as a normal distribution with mean = 4750 cm^2 and SD = 750 cm^2. Indoor temperatures in the base case were calculated adding this probability distribution to the methodology described above (Fig. 8). Most of the measurements were not in the range of "calculated hourly indoor temperature ± 2SD" (Fig. 8). Despite this negative result, calculated values and measured values were arguably similar enough to consider the model calibration adequate.

In the base case, 44% of discomfort time during a year was calculated. Five non-dominated solutions in terms of investment costs and discomfort were found (Fig. 9). The minimum percentage of discomfort time during a year was 37% after investing 286 USD in adding insulated door and adding insulated roof (Table 6). 84 out of the 215 tested designs had discomfort time lower than the base case. The importance of decreasing the roof transmissivity is notorious because the solution *adding insulated roof* was present in 73% of these 84 designs.

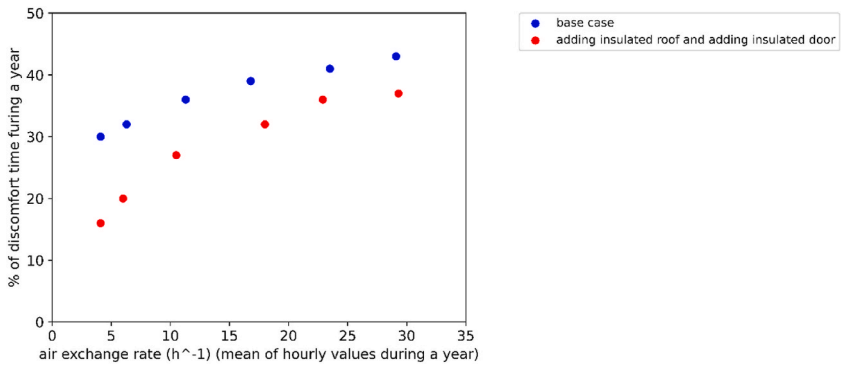

Fig. 10. Effect of reducing infiltration in discomfort time for the base case and the design combining adding insulated roof and adding insulated door.

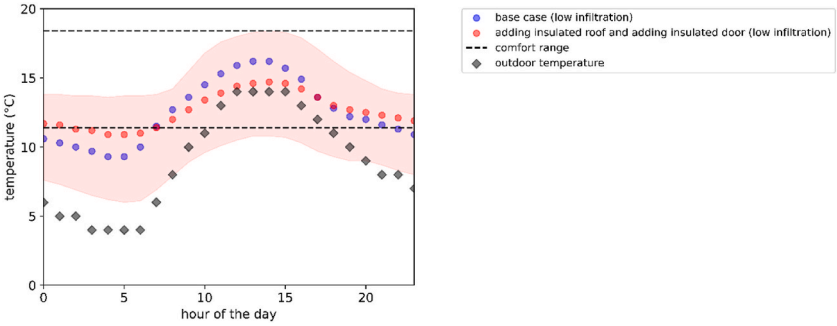

Fig. 11. Indoor air temperatures after reducing infiltration to 4.1 h^{-1}. Dots are mean of hourly values during a year, and shadowed area is the distribution between percentiles 5th and 95th.

Investing in retrofitting did not necessarily decrease discomfort (Fig. 9), 131 of the 215 tested designs had discomfort times equal or higher than the base case. The highest discomfort time was 50% and it belonged to the design combining adding shutter to the window, adding walls interior insulation to walls, adding insulated floor, and adding skylight. *Adding insulated floor* was the solution most present among of these 131 designs, it was present in 56% of the designs. However, it's effect over the discomfort time was not necessarily negative because it also was present in a similar proportion (42%) among the solutions with lower discomfort time than the base case.

The mean value of the hourly air exchange rate (AER) in the base case after calibration was 29.1 h^{-1} (SD = 17.0 h^{-1}), and in the solution with the lowest discomfort (combining *adding insulated roof* and *adding insulated door*) was 29.3 h^{-1} (SD = 17.5 h^{-1}) (Fig. 10). These high AER are a consequence of high $A_L = 4500$ cm^2 (SD = 750 cm^2) and low room volume. An infiltration sensitivity analysis was done; the A_L mean value until a mean AER equal 4.1 h-1 (SD = 4.1 h-1) was reached. With this level of infiltration, the minimum discomfort time was 16%. The calculated comfort temperatures (T_c in Eq (3)), was 14.9 °C. Considering a comfortable range of ±3.5 °C, the design with adding insulated roof and adding insulated door had only cold discomfort (Fig. 11).

4. Discussion

Our study indicates that the lowest discomfort time is obtained after adding insulated roof and adding insulated door. The decrement of discomfort was 7% (613 h during a year) in comparison with the base case and an investment of 286 USD was needed. The base case can also improve with lower investment but lower decrement of discomfort. We have not found references to discuss a desirable ratio between discomfort reduction per invested dollar, but we believe that the goal should be zero discomfort time. In the studied context, the reduction of discomfort is limited by the low investment capacity of the households.

Measure to decrease infiltration decreased discomfort in both the base case and in the design combining *adding insulated roof* and *adding insulated door*. Reducing infiltration in the base case reduced discomfort more than *adding insulated roof* and *adding insulated door,* 14% and 7% respectively. However, suggesting measures to reduce infiltration and their impact on the air exchange rate was out of the scope of this study. In addition, impact of low infiltration on human health, and on the moisture content of adobe walls have to be considered. Other researchers have also recommended the combination of infiltration reduction and roof insulation, such as those mentioned in the reference documents [15,16,74]. However, cold discomfort persisted in low infiltration levels, suggesting that other measurements should be included to improve these houses, e.g., roof with lower transmittance, passive heating techniques, or mechanical heating systems, such as in reference document [6].

Some modifications to the base case increased discomfort time, and, in other cases, more investment did not decreased discomfort. Thus, our results raised awareness about the importance of combining well-intended actions with numerical calculations. These approach is important especially in public housing programs that refurbish or build thousands of houses.

Unlike other previous calculations of comfort in the Peruvian mountains [6,75], our work used an adaptive model developed for people living in Nepalese mountains with low indoor temperatures. This model defines a comfortable range with lower temperatures than those of other adaptive thermal comfort model such as De Dear & Brager's [19] model used in reference document [75]. Using a different comfort model would lead to different optimal solutions. We chose the Nepalese research because of the similar living conditions but there are other models developed for people living in high altitude mountains such as the aPMV model tested in field experiments for residential buildings [23,27]. It is important to do thermal comfort surveys for the rural Andean population in Peru to improve the evaluation of retrofitting solutions.

The inclusion of a variety of conditions in our calculations made our results robust but also increased the uncertainty of the output. Some uncertainties are sparsely documented in the literature, such as effective air leakage areas, building layouts, internal heat gains, or the thermal properties of the local adobes. Further research will help to decrease the output's uncertainty.

One of these uncertainties having significant importance on the calculations was infiltration. Two previous studies have modelled rural houses in the Peruvian mountains [6,16] using EnergyPlus. These researchers modelled houses with a constant infiltration of 1 h^{-1}. We consider that a transient calculation of the infiltration (Eq (3)) is closer to reality. However, in one of those studies [6], indoor

temperature calculations were compared with actual measurements, and the difference was less than 1 °C during nighttime hours; nevertheless, that studied building appeared to be more airtight than the traditional houses.

5. Conclusions

In this study, we numerically calculated the impact of 9 refurbishing solutions to decrease discomfort time in rural houses in the Peruvian mountains. The solutions were defined as modifications to a typical one-room hut by adding insulation to a surface or adding a skylight. The information for a typical one-room hut was the base case scenario. The base case had a metal-sheet roof, adobe walls, dirt floor, and significant infiltration. Infiltration levels were approximated calibrating an EnergyPlus model with field measurements. The application of one or more solutions to the base case transformed the base case into 215 new house designs. Energyplus was used to calculated discomfort time during a year. The calculations included an uncertainty analysis of all inputs and a sensitivity analysis of air infiltration.

In conclusion, to help the inhabitants affected by uncomfortable indoor temperatures, we recommend promoting the adding of insulation to the roof ($U = 0.83\ W/m^2 \bullet K$) and to the door ($U = 1.00\ W/m^2 \bullet K$) with an investment of 286USD. This was the solution that produced the lowest discomfort during a year, 37% of the time, among the calculated optimal solutions in terms of discomfort time and costs. Other four solutions formed the Pareto front and they are also recommended in cases when less expensive solutions are required. Our results showed that 61% of the tested designs had none or a negative impact on the discomfort time.

By calibrating an EnergyPlus model with eight-days measurements of a typical hut, it was found that hourly air exchange rate (AER) levels with mean equal to 29.1 h^{-1} (SD = 17.0 h^{-1}) reduced the error between the measurements and the calculations to adequate levels. Reducing infiltration reduced discomfort in both the base case and the solution with added insulation to the roof and the door. In the latter solution, discomfort time was reduced until 16%. when mean hourly AER was equal to 4.1 h-1 (SD = 4.1 h-1). All this discomfort time was cold discomfort. Specific measures to reduce infiltration were not listed because of lack of information about their impact.

Although this was a theoretical study, the calculations offer relevant information regarding the households in relation to current actions being implemented to improve their housing conditions. Most households have limited economic resources to invest in refurbishing, and this situation limits the number of refurbishing solutions that they can afford. Households should continue making an effort to reduce infiltration, and prioritize investments by adding insulation to roofs and doors.

Author contribution statement

Enrique Mejia Solis: Conceived and designed the experiments; Performed the experiments; Analyzed and interpreted the data; Contributed reagents, materials, analysis tools or data; Wrote the paper.

Björn Palm: Jaime Arias: Analyzed and interpreted the data.

Data availability statement

No data was used for the research described in the article.

Additional information

During this study, Enrique Mejia-Solis had a scholarship for his PhD studies granted by Peru's National Counsil of Science, Technology, and Technological Innovation (CONCYTEC) with contract number 303-2014-FONDECYT.

Declaration of competing interest

The authors declare that they have no known competing financial interests or personal relationships that could have appeared to influence the work reported in this paper.

References

[1] T. Alejandro, Sistema constructivo para viviendas rurales, in: Simposio de innovación y desarrollo de nuevas tecnologías, 2019/01/31/, 2019. Ministerio de vivienda, construcción y saneamiento. [Online]. Available: http://dgadt.vivienda.gob.pe/Eventos/SimposioPonencias http://dgadt.vivienda.gob.pe/Eventos/SimposioPonencias [Online]. Available:.

[2] C. Jiménez, M. Wieser, S. Biondi, Improving thermal performance of traditional cabins in the high-altitude Peruvian andean region, in: Presented at the Passive and Low Energy Architecture, PLEA, Edinburgh, 2017.

[3] Á.C. Gutiérrez, G.B. Quispe, A.P.C. Mendoza, H.N.C. Betancur, E.H. Ramos, Confort térmico y el riesgo de infecciones respiratorias en los adultos mayores en la sierra rural del Perú, Rev. Española Geriatría Gerontol. 56 (1) (2021) 24–28.

[4] M.d.P. Gayoso, O.C. Pacheco, Análisis tipológico de vivienda alpaquera altoandina como base para creación de nuevos modelos: Caso de estudio en Puno-Perú, Instituto de arquitectura tropical, 2015.

[5] P.R.D. Williams, K. Unice, Field study of air exchange rates in northern highlands of Peru (in eng), Environ. Forensics 14 (3) (2013 2013) 215–229, https://doi.org/10.1080/15275922.2013.814182.

[6] J. Molina, R. Espinoza, M. Horn, M. Gómez, Thermal performance evaluation of isolation and two active solar heating systems for an experimental module: a rural Peruvian case at 3700 masl, J. Phys. Conf. 1173 (1) (2019), 012003. IOP Publishing.

[7] F. Lima, P. Ferreira, V. Leal, A review of the relation between household indoor temperature and health outcomes, Energies 13 (11) (2020) 2881, https://doi.org/10.3390/en13112881.
[8] 2019). Plan Multisectorial ante Heladas y Friaje 2019-2021. [Online] Available: https://cdn.www.gob.pe/uploads/document/file/350878/Plan_Multisectorial_ante_Heladas_y_Friaje_2019_COMPLETO_FINAL_TRIMBOX.pdf.
[9] I. Instituto Nacional de Estadística e, "Perú: Encuesta Demográfica de Salud Familiar ENDES 2016," ed: Instituto Nacional de Estadística e Informática (INEI), 2017..
[10] S. Rutstein, G. Rojas, Guide to DHS Statistics, United States Agency for International Development (USAID), 2006.
[11] Perú: perfil sociodemográfico. Informe nacional. Censos nacionales 2017: XII de Población, VII de Vivienda y III de Comunidades indígenes [Online] Available: https://www.inei.gob.pe/media/MenuRecursivo/publicaciones_digitales/Est/Lib1539/libro.pdf, , 2018.
[12] S. Ministerio de Desarrollo e Inclusión, "Mi Abrigo," ed..
[13] J. Soria, M. Hadzich, C. Hadzich, V. Ramos, "Casa caliente limpia PUCP: modelo sostenible de un sistema de confort térmico frente al fenómeno de las heladas.," presented at the I Congreso de energías renovables y arquitectura bioclimática CABER 2017, 2017. Lima - Perú.
[14] Evaluación de impacto de la primera fase de "Mi abrigo"- Línea de base [Online] Available: http://evidencia.midis.gob.pe/evaluacion-de-impacto-de-la-primera-fase-de-mi-abrigo-linea-de-base/, 2017.
[15] Ministerio de Vivienda Construcción y Saneamiento del Perú and Deutsche Gesellschaft für Internationale Zusammenarbeit, in: Abrigando Hogares: Experiencias con medidas de confort térmico en viviendas rurales altoandinas, 2015.
[16] M. Wieser, S. Onnis, G. Meli, Desempeño térmico de cerramientos de tierra alivianada : posibilidades de aplicación en el territorio peruano, Rev. Arquit. 22 (1) (2020) 164–174, https://doi.org/10.14718/RevArq.2020.2633.
[17] M. Wieser, S. Rodriguez-Larrain, S. Onnis, Bioclimatic strategies for high altitude tropical cold climate. Prototype validation in Orduna, Puno, Peru (in Spanish), ESTOA-REVISTA DE LA FACULTAD DE ARQUITECTURA Y URBANISMO DE LA UNIVERSIDAD DE CUENCA 10 (19) (2021) 9–19, https://doi.org/10.18537/est.v010.n019.a01. JAN-JUL.
[18] J.R. Molina, G. Lefebvre, R. Espinoza, M. Horn, M.M. Gomez, Bioclimatic approach for rural dwellings in the cold, high Andean region: a case study of a Peruvian house, Energy Build. 231 (JAN 15 2021), https://doi.org/10.1016/j.enbuild.2020.110605 (in English).
[19] R. De Dear, G.S. Brager, Developing an adaptive model of thermal comfort and preference, Build. Eng. 104 (1) (1998).
[20] A. Holguino, L. Olivera, K.U. Escobar, Confort térmico en una habitación de adobe con sistema de almacenamiento de calor en los andes del Perú, Revista de Investigaciones Altoandinas 20 (3) (2018 2018) 289–300 [Online]. Available: http://www.scielo.org.pe/scielo.php?pid=S2313-29572018000300003&script=sci_abstract&tlng=en.
[21] I. Miño-Rodríguez, C. Naranjo-Mendoza, I. Korolija, Thermal assessment of low-cost rural housing—a case study in the Ecuadorian Andes, Buildings 6 (3) (2016) 36, https://doi.org/10.3390/buildings6030036.
[22] R. Thapa, H.B. Rijal, M. Shukuya, H. Imagawa, Study on the wintry thermal improvement of makeshift shelters built after Nepal earthquake 2015, Energy Build. 199 (2019/09/15/2019) 62–71, https://doi.org/10.1016/j.enbuild.2019.06.031.
[23] W. Yu, B. Li, R. Yao, D. Wang, K. Li, A study of thermal comfort in residential buildings on the Tibetan Plateau, China, Build. Environ. 119 (2017/07/01/2017) 71–86, https://doi.org/10.1016/j.buildenv.2017.04.009.
[24] H.B. Rijal, H. Yoshida, Winter thermal comfort of residents in the Himalaya region of Nepal, in: Proceeding of International Conference on Comfort and Energy Use in Buildings-Getting Them Right, Windsor), 2006, pp. 1–15.
[25] G.S. Brager, R.J. de Dear, Thermal adaptation in the built environment: a literature review, Energy Build. 27 (1) (1998/02/01/1998) 83–96, https://doi.org/10.1016/S0378-7788(97)00053-4.
[26] M.A. Humphreys, H.B. Rijal, J.F. Nicol, Updating the adaptive relation between climate and comfort indoors; new insights and an extended database, Build. Environ. 63 (2013/05/01/2013) 40–55, https://doi.org/10.1016/j.buildenv.2013.01.024.
[27] B. Cheng, Y. Fu, M. Khoshbakht, L. Duan, J. Zhang, S. Rashidian, Characteristics of thermal comfort conditions in cold rural areas of China: a case study of stone dwellings in a Tibetan village, Buildings 8 (4) (2018) 49, https://doi.org/10.3390/buildings8040049.
[28] S. Chang, W.R. Santee, Clothing insulation in a hypobaric environment, Aviat Space Environ. Med. 67 (9) (1996) 827–834.
[29] J. Molina, V. Nakama, G. Lefebvre, A low-cost measurement device for recording perceptions of thermal comfort, in: Journal of Physics: Conference Series vol. 1433, IOP Publishing, 2020, 012006, 1.
[30] V.H. Reynoso Achahuanco, Impacto del programa nacional de vivienda rural en la calidad de vida de los beneficiarios en los centros poblados de Llanca y Quillisani – Paratia – Lampa - Puno 2018, Bachellor Thesis, Universidad Nacional de San Agustín de Arequipa, Arequipa, Peru, 2019 [Online]. Available: http://repositorio.unsa.edu.pe/handle/UNSA/8496.
[31] R. Thapa, H.B. Rijal, M. Shukuya, Field study on acceptable indoor temperature in temporary shelters built in Nepal after massive earthquake 2015, Build. Environ. 135 (2018/05/01/2018) 330–343, https://doi.org/10.1016/j.buildenv.2018.03.001.
[32] F. Ordóñez, F. Jácome, P. Castro, C. Naranjo-Mendoza, Sensitivity analysis of the variables affecting indoor thermal conditions on unconditioned dwellings in equatorial high-altitude regions from an experimentally validated model, Adv. Build. Energy Res. 15 (4) (2021) 442–465, https://doi.org/10.1080/17512549.2019.1582437, 2021/07/04.
[33] Z. Pang, Z. O'Neill, Y. Li, F. Niu, The role of sensitivity analysis in the building performance analysis: a critical review, Energy Build. 209 (2020), 109659, https://doi.org/10.1016/j.enbuild.2019.109659, 2020/02/15.
[34] D.B. Crawley, et al., EnergyPlus: creating a new-generation building energy simulation program, Energy Build. 33 (4) (2001/04/01/2001) 319–331, https://doi.org/10.1016/S0378-7788(00)00114-6.
[35] American society of heating refrigerating air conditioning engineers, in: 2017 ASHRAE Handbook-Fundamentals, 2017.
[36] U.S. Department of Energy, EnergyPlus Version 9.1.0 Documentation: Engineering Reference, U.S. Department of Energy, 2019.
[37] N. Kruis, M. Krarti, KivaTM: a numerical framework for improving foundation heat transfer calculations, Journal of Building Performance Simulation 8 (6) (2015) 449–468, https://doi.org/10.1080/19401493.2014.988753.
[38] T.R. Oke, Boundary Layer Climates, Psychology Press, 1987, p. 460 (in en).
[39] Instituto Nacional de Estadística e Informática del Perú, Perú, ed, 2020, Encuesta Demográfica de Salud Familiar ENDES, 2019.
[40] EM 110, Confort térmico y lumínico con eficiencia energética, Ministerio de vivienda construcción y saneamiento del Perú, 2014.
[41] C.J. Hopfe, J.L.M. Hensen, Uncertainty analysis in building performance simulation for design support, Energy Build. 43 (10) (2011/10/01/2011) 2798–2805, https://doi.org/10.1016/j.enbuild.2011.06.034.
[42] A. Chong, W. Xu, K.P. Lam, Uncertainty analysis in building energy simulation-a practical approach, in: J. Mathur, V. Garg (Eds.), 14th International IBPSA Conference, 2015, pp. 2796–2803.
[43] K.J. Lomas, H. Eppel, Sensitivity analysis techniques for building thermal simulation programs, Energy Build. 19 (1) (1992/01/01/1992) 21–44, https://doi.org/10.1016/0378-7788(92)90033-D.
[44] C. Spitz, L. Mora, E. Wurtz, A. Jay, Practical application of uncertainty analysis and sensitivity analysis on an experimental house, Energy Build. 55 (2012/12/01/2012) 459–470, https://doi.org/10.1016/j.enbuild.2012.08.013.
[45] W.A. Mahar, G. Verbeeck, S. Reiter, S. Attia, Sensitivity analysis of passive design strategies for residential buildings in cold semi-arid climates, Sustainability 12 (3) (2020) 1091 [Online]. Available: https://www.mdpi.com/2071-1050/12/3/1091.
[46] G. Calleja Rodríguez, A. Carrillo Andrés, F. Domínguez Muñoz, J.M. Cejudo López, Y. Zhang, Uncertainties and sensitivity analysis in building energy simulation using macroparameters, Energy Build. 67 (2013/12/01/2013) 79–87, https://doi.org/10.1016/j.enbuild.2013.08.009.
[47] V.A.C.D. Costa, V.F. Roriz, K.M.S. Chvatal, Modeling of slab-on-grade heat transfer in EnergyPlus simulation program, Ambiente Construído 17 (3) (2017 2017) 117–135, https://doi.org/10.1590/s1678-86212017000300166.
[48] M. Pfundstein, R. Gellert, M. Spitzner, A. Rudolphi, Insulating Materials: Principles, Materials, Applications, Walter de Gruyter, 2012.
[49] T.A. Osswald, G. Menges, Materials Science of Polymers for Engineers, 3 ed., Carl Hanser Verlag GmbH & Co. KG, München, 2012 (in en).

[50] H. Suehrcke, E.L. Peterson, N. Selby, Effect of roof solar reflectance on the building heat gain in a hot climate, Energy Build. 40 (12) (2008/01/01/2008) 2224–2235, https://doi.org/10.1016/j.enbuild.2008.06.015.
[51] 14. pr ed.R.E.T. Bolz, L. George, R.E. Bolz, G.L. Tuve (Eds.), CRC Handbook of Tables for Applied Engineering Science, second ed., CRC Press, Boca Raton, Florida, 2000, p. 1166 (in eng)
[52] M. Wieser Rey, Consideraciones bioclimáticas en el diseño arquitectónico: el caso peruano, in: Lima: Centro de Investigación de la Arquitectura y la Ciudad, Pontificia Universidad Católica del Perú, 2011.
[53] E. Mazria, The Passive Solar Energy Book: a Complete Guide to Passive Solar Home, Greenhouse and Building Design, Emmaus, Pa, Emmaus, Pa, 1979, p. 435 (in eng).
[54] J.D. Balcomb, Heat Storage and distribution inside passive solar buildings, in: S. Yannas (Ed.), Passive and Low Energy Architecture, Pergamon, 1983, pp. 547–561.
[55] G. Minke, Building with Earth: Design and Technology of a Sustainable Architecture, Walter de Gruyter GmbH, Basel: Basel, 2006.
[56] G.A. Abanto, M. Karkri, G. Lefebvre, M. Horn, J.L. Solis, M.M. Gómez, Thermal properties of adobe employed in Peruvian rural areas: experimental results and numerical simulation of a traditional bio-composite material, Case Stud. Constr. Mater. 6 (2017/06/01/2017) 177–191, https://doi.org/10.1016/j.cscm.2017.02.001.
[57] H.B. Rijal, Thermal adaptation of buildings and people for energy saving in extreme cold climate of Nepal, Energy Build. 230 (2021/01/01/2021), 110551, https://doi.org/10.1016/j.enbuild.2020.110551.
[58] Z. Lin, S. Deng, A study on the thermal comfort in sleeping environments in the subtropics—measuring the total insulation values for the bedding systems commonly used in the subtropics, Build. Environ. 43 (5) (2008/05/01/2008) 905–916, https://doi.org/10.1016/j.buildenv.2007.01.027.
[59] U.S. Department of Energy, EnergyPlus Version 9.3.0 Documentation: Engineering Reference, U.S. Department of Energy, 2020.
[60] M. Sleiman, et al., Soiling of building envelope surfaces and its effect on solar reflectance—Part I: analysis of roofing product databases, Sol. Energy Mater. Sol. Cell. 95 (12) (2011/12/01/2011) 3385–3399, https://doi.org/10.1016/j.solmat.2011.08.002.
[61] D. Gürlich, A. Reber, A. Biesinger, U. Eicker, Daylight performance of a translucent textile membrane roof with thermal insulation, Buildings 8 (9) (2018), https://doi.org/10.3390/buildings8090118.
[62] J. Nijskens, J. Deltour, S. Coutisse, A. Nisen, Radiation transfer through covering materials, solar and thermal screens of greenhouses, Agric. For. Meteorol. 35 (1) (1985/10/01/1985) 229–242, https://doi.org/10.1016/0168-1923(85)90086-3.
[63] J. Hu, X. Yu, Design and characterization of energy efficient roofing system with innovative TiO2 enhanced thermochromic films, Construct. Build. Mater. 223 (2019/10/30/2019) 1053–1062, https://doi.org/10.1016/j.conbuildmat.2019.06.003.
[64] J. Nijskens, J. Deltour, S. Coutisse, A. Nisen, Heat transfer through covering materials of greenhouses, Agric. For. Meteorol. 33 (2–3) (1984) 193–214.
[65] X. Yin, Y. Zhang, J. Zhang, Transparent plasticised PVC film with ultraviolet and high-energy visible light shielding performance, Plast., Rubber Compos. 46 (9) (2017) 375–380.
[66] Y. Qi, X. Yin, J. Zhang, Transparent and heat-insulation plasticized polyvinyl chloride (PVC) thin film with solar spectrally selective property, Sol. Energy Mater. Sol. Cell. 151 (2016) 30–35, https://doi.org/10.1016/j.solmat.2016.02.016, 2016/07/01/.
[67] F.P. Incropera, D.P. DeWitt, Fundamentals of Heat and Mass Transfer, fourth ed., John Wiley & Son, 1996.
[68] S. Schare, K.R. Smith, Particulate emission rates of simple kerosene lamps, Energy for Sustainable Development II (2) (1995 1995) 33–35.
[69] J.P. McCracken, K.R. Smith, Emissions and efficiency of improved woodburning cookstoves in Highland Guatemala, Environ. Int. 24 (7) (1998/10//1998) 739–747, https://doi.org/10.1016/S0160-4120(98)00062-2.
[70] D.K. Shahi, H.B. Rijal, G. Kayo, M. Shukuya, Study on wintry comfort temperature and thermal improvement of houses in cold, temperate, and subtropical regions of Nepal, Build. Environ. 191 (2021), 107569, https://doi.org/10.1016/j.buildenv.2020.107569, 2021/03/15/.
[71] B. Gautam, H.B. Rijal, M. Shukuya, H. Imagawa, A field investigation on the wintry thermal comfort and clothing adjustment of residents in traditional Nepalese houses, J. Build. Eng. 26 (2019), 100886, https://doi.org/10.1016/j.jobe.2019.100886, 2019/11/01/.
[72] H.B. Rijal, H. Yoshida, N. Umemiya, Seasonal and regional differences in neutral temperatures in Nepalese traditional vernacular houses, Build. Environ. 45 (12) (2010) 2743–2753, https://doi.org/10.1016/j.buildenv.2010.06.002, 2010/12/01/.
[73] American society of heating refrigerating air conditioning engineers, in: ASHRAE Standard 55: Thermal Environmental Conditions for Human Occupancy, 2017.
[74] J.J. Natividad Alvarado, D. Ocupa Florián, M. Horn, "¿Los muros de Trombe sirven en el Perú?," presented at the IV Conferencia Latino Americana de Energía Solar (IV ISES_CLA) y XVII Simposio Peruano de Energía Solar (XVII- SPES), 2010. Cusco.
[75] M. Wieser, S. Onnis, and G. Meli, "Desempeño térmico de cerramientos de tierra alivianada. Posibilidades de aplicación en el territorio peruano Thermal performance of light earth building envelope. Possibilities of application in the Peruvian territory.".